Vol. 47: 29–47, 2022
https://doi.org/10.3354/esr01164

ENDANGERED SPECIES RESEARCH
Endang Species Res

Published January 13

Decomposition of Kemp's ridley (*Lepidochelys kempii*) and green (*Chelonia mydas*) sea turtle carcasses and its application to backtrack modeling of beach strandings

Redwood W. Nero[1], Melissa Cook[2,*], Jaymie L. Reneker[3], Zhankun Wang[4,5], Emma A. Schultz[3], Brian A. Stacy[6]

[1]National Oceanic and Atmospheric Administration, National Marine Fisheries Service, Southeast Fisheries Science Center, Building 1021, Stennis Space Center, Mississippi 39529, USA

[2]National Oceanic and Atmospheric Administration, National Marine Fisheries Service, Southeast Fisheries Science Center, Pascagoula, Mississippi 39567, USA

[3]Riverside Technologies Inc., Southeast Fisheries Science Center, Pascagoula, Mississippi 39567, USA

[4]National Oceanic and Atmospheric Administration National Centers for Environmental Information, Stennis Space Center, Mississippi 39529, USA

[5]Northern Gulf Institute, Mississippi State University, Stennis Space Center, Mississippi 39529, USA

[6]National Oceanic and Atmospheric Administration, National Marine Fisheries Service, Office of Protected Resources, University of Florida, College of Veterinary Medicine (duty station), Gainesville, Florida 32611, USA

ABSTRACT: When a sea turtle dies, it typically sinks to the bottom, begins decomposing, and floats to the surface once sufficient internal gases have accumulated to produce positive buoyancy. This process is poorly characterized and is essential to understanding where and when sea turtles found on shore may have died. We conducted decomposition studies with detailed time–temperature histories using carcasses of cold-stunned sea turtles (22 Kemp's ridleys *Lepidochelys kempii* and 15 green sea turtles *Chelonia mydas*) at temperatures of 14–32°C and depths of 2.2–9.5 m. We found strong depth/pressure-related effects; carcasses took longer to float when incubated at greater depths than shallower depths at similar temperatures. Furthermore, carcasses incubated at colder temperatures (~15°C) took 8 times longer to float than those at 32°C at the same depth. We applied accumulated degree hours (ADH; hourly sum of ambient temperatures a carcass experienced) to characterize environmental conditions associated with different stages of decomposition and key events, including buoyancy and sinking. A formula for temperature-correction of ADH was calculated to fit a nonlinear increase in decomposition at higher temperatures. These data were then used to improve an existing backtracking model by incorporating water temperature, depth (pressure), bathymetry, and postmortem condition. Heat maps of the probable mortality locations from the model agreed well with carcass and effigy drift experiments, demonstrating the overall reliability of the enhanced model. Our method can be used to estimate at-sea locations where sea turtles found washed ashore in the northern Gulf of Mexico likely died and may help inform similar efforts in other regions.

KEY WORDS: Carcass decomposition · Backtrack model · Sea turtle · Strandings · Endangered species

1. INTRODUCTION

Sea turtle carcasses found on shore, i.e. strandings, are one of the few indicators of mortality at sea. Predicting the location where shore-cast carcasses originally died is paramount to understanding sources of mortality and is especially important in wildlife management and conservation if the mortality sources are anthropogenic in origin. State of decomposition in combination with temperature and current veloc-

*Corresponding author: melissa.cook@noaa.gov

Publisher: Inter-Research · www.int-res.com

ity data from ocean hydrodynamic models can be used to numerically backtrack the path of a stranded sea turtle and hypothesize the likely location of death (Nero et al. 2013). The state of decomposition is likely inversely related to the ambient temperature experienced by a carcass, as rates of autolysis and bacterial decomposition are generally faster at higher temperatures (Vass 2001, Megyesi et al. 2005). Very little information exists on the decomposition of sea turtles, although several recent studies provide new insights for various sea turtle species (Nero et al. 2013, Santos et al. 2018, Cook et al. 2020, B. Higgins et al. unpubl. data).

A sea turtle will either float or sink upon its death. The cause of death influences which situation occurs. Sea turtles that die from sudden causes of mortality, such as forced submergence or a vessel strike, will likely sink initially, as has been documented in drowned sea turtles removed from fishing gear (Epperly et al. 1996). Conversely, any condition where there is air trapped in the body to the extent that it remains positively buoyant could result in floating at death. Such conditions include disease states or injuries involving the lung or gastrointestinal tract, pneumocoelom (air within the coelomic cavity), and severe gas embolism (García-Párraga et al. 2014, Parga et al. 2020).

Dead sea turtles that sink to the sea floor begin decomposing and then float to the sea surface if enough internal gases accumulate. The time required to decompose and eventually float varies greatly depending on water temperature and depth (influence of water pressure) and can add to the uncertainty of backtracking to the source mortality location. According to Boyle's law, gas volume is reduced by half for every doubling of pressure experienced by a submerged carcass. For example, at 10 m a carcass would experience double the pressure it would at the surface and would presumably require twice the amount of gas to become positively buoyant.

Thus, accurate backtracking requires solving 2 related components: (1) the ocean drift and (2) the time to float (TTF) from an unknown depth. The TTF is the time from when the carcass sinks to when it becomes buoyant and floats to the surface. The ocean drift track is solved using reverse time particle tracking, or backtracking, with known rates of leeway (Nero et al. 2013). However, since the depth along the backtrack route is not known until the backtrack is determined, the likely source location and depth is a complex function of distance from shore (backtrack length) and the particular bathymetry encountered along the backtrack. Both must be solved simultaneously to achieve a scientifically defensible backtrack prediction.

In this paper, we report on (1) laboratory decomposition experiments that inform backtracking and (2) provide an improved model that resolves the distance and depth components required for backtrack analysis. Controlled decomposition experiments are used to provide detailed measurements and analysis of the temperature-dependent TTF and decomposition rates for 2 species of sea turtle, Kemp's ridley *Lepidochelys kempii* and green sea turtle *Chelonia mydas*, under varying temperature and depth conditions. Since the main components of decomposition, autolysis and bacterial action, are both highly temperature dependent, a curvilinear temperature model is used. A depth-dependent Boyle's law correction is also proposed based on the time to achieve positive buoyancy as measured at deep (9.5 m) versus shallow (2.2 m) depths. Based on these inputs, we derive and demonstrate a time–temperature function and a numerical method for the depth–pressure dependency used to backtrack beach-stranded carcasses to the likely location where they died. Finally, we test the model by applying the routines to an extensive set of purposefully deployed carcass effigies and sea turtle carcasses in nearshore and offshore waters of coastal Mississippi (Cook et al. 2021).

2. MATERIALS AND METHODS

2.1. Ethics statement

This study was authorized under US Fish and Wildlife Service permit number TE 676395-5. No live animals were killed or harmed for this cadaver study.

2.2. Decomposition experiments

2.2.1. Carcasses

Sea turtle carcasses for determining the TTF and subsequent decomposition rates were obtained from the Massachusetts, Mississippi, Texas, and North Carolina Sea Turtle Stranding and Salvage Network (STSSN) (Table S1 in the Supplement at www.int-res.com/articles/suppl/n047p029_supp.pdf). The first 23 carcasses, used for the 2016 and 2017 trials, were cold-stunned sea turtles that were initially found alive but subsequently died. Sea turtles were promptly frozen (less than 0°C) once death was confirmed until they were shipped overnight to the Sten-

nis Space Center (SSC) site of the Mississippi Laboratories, NOAA Southeast Fisheries Science Center, where they were kept frozen until needed for experiments. All carcasses were used for experiments no later than 1 yr after death. In late 2017 and early 2018, an additional 14 carcasses (7 Kemp's ridleys and 7 green sea turtles) were salvaged from cold stun events and either frozen or kept refrigerated for a previously published study comparing the effects of freezing on decomposition (Cook et al. 2020). Freezing appears to have no significant impact on the TTF and decomposition rates (Cook et al. 2020), thus these additional carcasses were included in our analyses in order to maximize the sample size.

Frozen carcasses were first thawed in a freshwater bath and warmed to ~4°C over a period of 1–2 h prior to the initiation of observations of decomposition. A total of 37 carcasses (Table S1) were placed into tanks of freshwater until they floated, and were then transferred to protected outdoor pens to complete the decomposition process. There were some differences in the facilities and ambient conditions among years of study due to the availability of large-capacity tanks and specific study objectives.

2.2.2. 2016 decomposition trials

The first set of 7 trials was conducted during May to July 2016 in a 9.75 m (388 m^3) deep freshwater tank. Because experiments were conducted in freshwater, the model applications use a multiplier to convert freshwater density to the density of seawater. The density difference is a function of water temperature and salinity and is relatively small. The 9.75 m of freshwater is equivalent to 9.5 m of pressure in seawater. This tank was housed in a non-climate-controlled indoor facility at SSC; however, the tank remained generally cool relative to the surrounding ambient temperature, as it was located out of direct sunlight. Tank temperatures ranged from 19°C in May to about 27°C in July. Only Kemp's ridley carcasses were used in this experiment. Trials were conducted individually, one carcass at a time (designated K01 to K07, Table S1).

2.2.3. 2017 decomposition trials

A second set of experiments was completed in May through June 2017. These trials were conducted in a 1173 l (81 cm wide × 234 cm high) polyethylene water storage carboy set up within the same facility at SSC because the previously used tank was no longer in service. The carboy was covered in a 0.10 m layer of fiber insulation to reduce thermal swings from the ambient air conditions, and the depth of water was 2.31 m. Using the conversion described above, the density difference equates to approximately 2.20 m of seawater. Temperatures ranged from 14 to 32°C and were maintained by a chiller and heaters as necessary. Water flow from the pump kept water in the carboy well mixed. Eight Kemp's ridley and 8 green sea turtles were used over the course of 8 paired trials (Kemp's ridley paired with a green sea turtle), designated K08–K22 (Kemp's ridley, even numbers) and G09–G23 (green sea turtle, odd numbers) (Table S1).

2.2.4. 2017–2018 decomposition trials

A final set of experiments comparing unfrozen and frozen carcasses (reported by Cook et al. 2020) was conducted in this same carboy during December 2017 through January 2018. This was accomplished over 2 trials as groups of 4 unfrozen and 3 frozen carcasses of the same species. Trial 1 consisted of 7 Kemp's ridley sea turtles designated K24–K30 (Table S1). Trial 2 consisted of 7 green sea turtles designated G31–G37 (Table S1). Temperatures were maintained near 20°C using the same methods described above (see also Cook et al. 2020).

2.2.5. Monitoring and post float observations

In all trials, temperature was monitored manually with a YSI-85 Handheld Dissolved Oxygen, Conductivity, Salinity and Temperature System. Additionally, the first 7 trials were monitored digitally with Seamon time–depth recorders (TDRs). The TDRs were calibrated against routine measurements using the YSI-85 during each trial. Submerged carcasses (Table S1) were monitored with a Mobius ActionCam HD digital camera, set on a 1 min time-lapse mode, either mounted outside the tank to view the carcass through a glass viewing port, or in the case of the carboy, by viewing down into the bottom from the water surface.

Once carcasses floated to the surface, they were transferred to outdoor floating pens at Bay-Waveland Yacht Club harbor (30° 19′ 30″ N, 89° 19′ 32″ W) to complete decomposition. The exception were 2 carcasses (K01 and K02) at the beginning of the study where initial attempts to use indoor facilities for post-floating phases of decomposition failed to provide

appropriate conditions. Carcass condition and temperature were recorded twice daily, in the morning and evening on most days. Carcass condition was recorded using the following previously developed criteria based on the degree of bloating and percentage of the carcass above the waterline: Code 2.1, first floating; 2.2, moderate bloat; 3.1, fully bloated (i.e. peak floating); 3.2, post bloat; 3.3, sinking; 4, heavily decomposed; and 5, bare bones (Reneker et al. 2018; see the Appendix). In order to ensure that our backtracking method is applicable to general sea turtle stranding data, we also applied a more general carcass condition classification system used by the STSSN: fresh dead or mildly decomposed (Code 1), moderately decomposed (Code 2), severely decomposed (Code 3), dried carcass (Code 4), and bones (Code 5). Hereafter, coding of decomposition stages follows Reneker et al. (2018) except when specifically referred to as STSSN coding.

2.2.6. Accumulated degree hours and modeling

We characterized decomposition using accumulated degree hours (ADH), which measures thermal energy input into the carcass during decomposition in order to standardize temperature on the rate of decomposition (Cook et al. 2020). ADH values were calculated by summing the hourly mean water temperatures at each stage of decomposition beginning when a carcass was placed in the tank through its duration in the harbor. Although carcasses were exposed to ambient air and water temperatures, only water temperature was considered relevant when calculating ADH. We made this choice because water has a much higher specific heat conductivity than air and is the primary driver of heat loss or gain in carcasses because they are always at least 50% submerged. As presented in Section 3, we found that the relationship between temperature, ADH, and decomposition was nonlinear, i.e. carcasses decomposed much faster when ADH was accrued at higher temperatures, thus we also derived a corrected ADH (cADH) that incorporated this temperature dependence (Text S1).

2.3. Comparative data

To corroborate findings from the tank and carboy experiments, we compared these results with those from a previously published study in which decomposed carcasses were deployed and tracked in the Gulf of Mexico to study carcass drift and fate ('deployment carcasses'; Reneker et al. 2018). Here, we briefly summarize the relevant methods from this work, which included a notable sample size.

The time and temperature required to float was determined for 104 cold-stunned sea turtle carcasses (78 green sea turtles and 26 Kemp's ridleys) used for drift experiments. During calendar year 2017, these carcasses were systematically thawed in holding tanks at near 20–25°C for up to 3 d until they first floated, then maintained near 18°C until used in drift experiments (Reneker et al. 2018). Time–temperature histories were recorded on Kestrel Drop digital recorders at 20 min intervals, then averaged to hourly values. These carcasses were not monitored via camera; therefore, an accurate TTF is unknown. Carcasses were checked every few hours during the day. While some were observed floating during the day, others were found floating in the morning. The estimated TTF included greater uncertainty than those determined by time-lapse video in the current study; however, observations were mostly within 12 h of the actual TTF and thus still provided a useful range for comparison purposes.

2.4. Drift experiments

The above deployment carcasses were used in carcass drift experiments to understand stranding seasonality (Cook et al. 2021). For the current study, we enhanced a backtrack model based on parameters from our decomposition studies and used the drifter experiment data to evaluate the ability of the model to predict the general location of the drop sites. Drift tracks from wooden effigies utilized by Cook et al. (2021) were also used to evaluate the accuracy of the model. Small, 2′ × 3′ × 1′ (5.1 × 7.6 × 2.5 cm) SPOT Trace GPS satellite transmitters (SPOT) provided real-time monitoring of locations and determination of the actual time objects reached land or if they were lost at sea.

A total of 182 carcasses and 100 effigies, hereafter referred to as 'objects,' were deployed at 3 sites (A, B, C), twice per month during the 2017 drift study (Cook et al. 2021). To maximize comparability of effigies and carcasses, only effigies with drift durations that did not exceed observed carcass decomposition rates were selected for backtracking. Only 46% (n = 120) of objects were included in the analysis. The remaining objects either vanished (possible scavenging or decomposition of carcasses or SPOT malfunction), were effigies that drifted beyond the persistence of an actual carcass, or were objects that were never recovered (Cook et al. 2021). Over half (n = 63) of

beached objects were deployed from inshore Site A, followed by 39 at intermediate Site B, and 18 from offshore Site C (Cook et al. 2021).

Predicted condition codes were calculated for effigies (n = 59) by first estimating the cADH at beaching. To do this, the cADH to float (cADHf) for each deployment site was calculated using deployment depth and bottom temperature obtained from NOAA Northern Gulf Ocean Forecast System (NGOFS) and Eqs. (2) & (3), defined in Section 3.1. This value was then added to the result of the sea surface temperature at deployment multiplied by the number of hours adrift to calculate the total predicted cADH at beaching. A condition code was then assigned to the effigy by comparing its predicted beaching cADH and the mean cADH for each condition code, derived from our carcass studies, and assigning it to the closest code (Cook et al. 2021). Carcass decomposition codes were also evaluated. If the carcass deployment condition code was 2.1 or 2.2 (n = 44), the actual beaching condition code when found was assigned. However, if the deployment condition code was 3.1 (n = 20), due to difficulties achieving carcass flotation, then the beaching condition code was also predicted in the same way as the effigies.

Backtrack modeling was carried out using the modeling algorithms described in Eqs. 1–11 in Section 3 and the numerical methods described by Nero et al. (2013), who downloaded oceanographic data from the NGOFS hydrodynamic model (https://tidesandcurrents.noaa.gov/ofs/ngofs/ngofs.html), with 15 min linearly interpolated time steps within the NGOFS hourly resolution. NGOFS is a 40-layer finite element model providing high resolution (200–300 m scale) within the complex coastal bays and estuaries out to a coarse resolution (~5–10 km scale) near the outer boundary of the model at the shelf edge. All computations were carried out using Matlab (The Math Works).

3. RESULTS

3.1. Decomposition experiments

3.1.1. TTF and temperature

Tank and carboy experiments produced the TTF for 37 carcasses. Most carcasses were maintained in the harbor until they sank and only bare bones remained; however, 4 carcasses (K03, K08, G09, and G14) were lost prior to becoming skeletonized due to either human interference or breaching of the sea pens by scavengers. Fig. 1 provides a detailed example of a time–temperature sequence of a single carcass (K04), from freshly thawed (Day 0), through first floating (3.7 d), sinking (9 d), and then decomposition to bare bones (10.5 d). Temperature and time data, presented in a similar way as for K04 above (Fig. 1), are shown for the first 23 trials conducted during the warmer spring and summer months (Fig. 2a), where each carcass is represented by a unique color, ranked by their initial temperature, from warmest (G21) to coolest (K10). TTF, peak float (90–100% of carapace exposed above the waterline, severely bloated, >3/4 of head and neck visible above waterline), time to sink, and bare bones are indicated as symbols on each line (Fig. 2a). Generally, the warmest trials decomposed the fastest, being complete in 5–10 d, while the coolest trials took up to 25 d.

The final group of 14 carcasses used in the frozen versus unfrozen experiments (Cook et al. 2020), was tested during winter months because of the limited availability of fresh carcasses at other times.

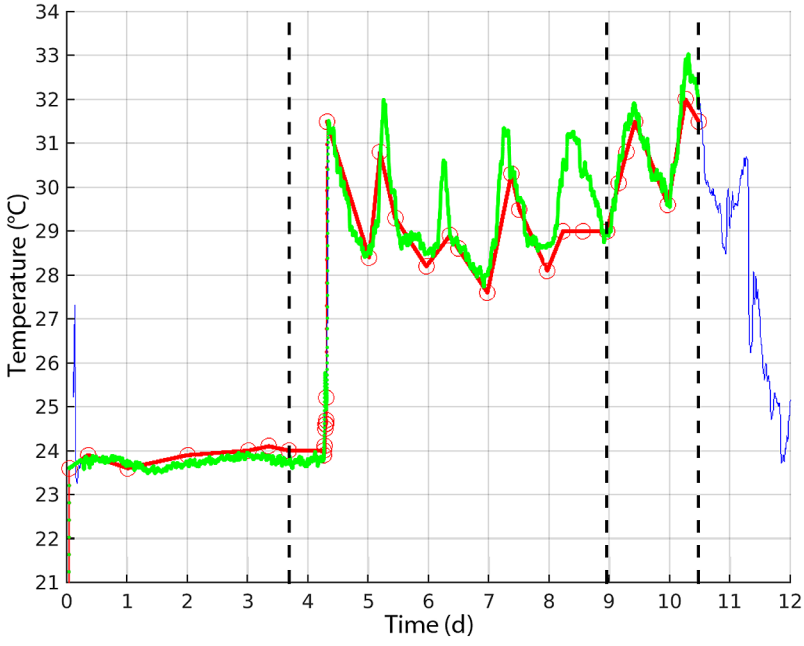

Fig. 1. Time–temperature observations of decomposition trial number 4 (Kemp's ridley K04), from the tank in 2016. Red circles and line: YSI-85 Handheld Dissolved Oxygen, Conductivity, Salinity and Temperature System measurements; blue line: Seamon time–depth recorder (TDR) measurements; green line: best fit of YSI and TDR data as used in the analysis. Vertical dashed lines designate observations of the time of float, sink, and decomposition to bare bones

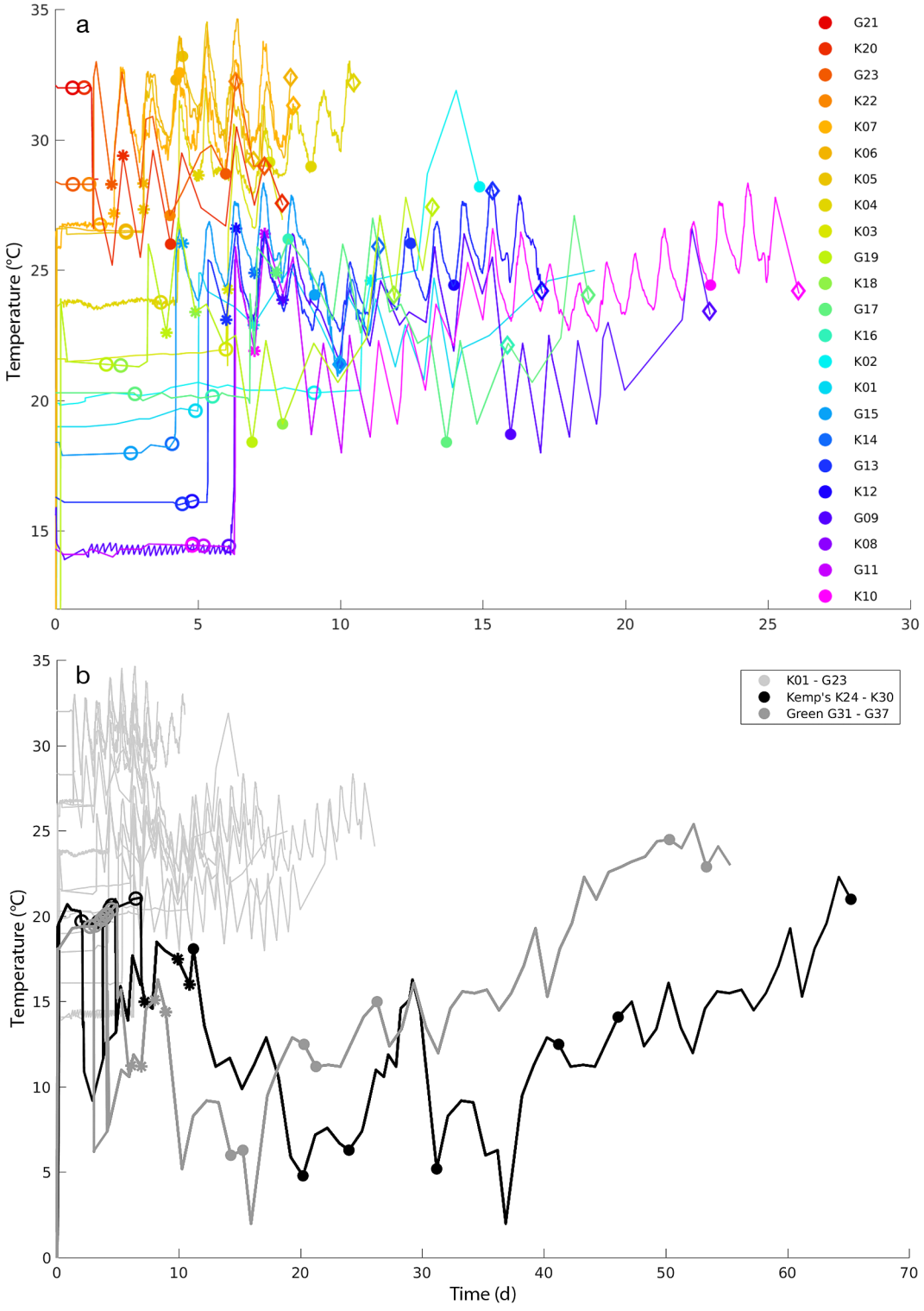

Fig. 2. (a) Summary of 23 decomposition trials with: 7 Kemp's ridley carcasses in the tank (K01–K07) and 16 carcasses in the carboy, of which 8 were Kemp's ridleys (K08–K22, even numbers), and 8 were green sea turtles (G09–G23, odd numbers). Line colors designate the approximate overall mean temperature at which experiments were initially conducted, ranging from cool (purple–blue) to warm (red). Open circles designate time of floating, asterisks mark peak float, filled circles indicate sinking, and diamonds represent the bare bones stage. (b) Summary of 14 additional cold-temperature decomposition trials shown on an extended time scale with: 7 Kemp's ridley carcasses (black curves) and 7 green sea turtle carcasses (medium grey). Marker symbols as in panel (a) but with the first 23 carcasses (warmer trials) in light grey to reduce clutter

Because of their longer duration in the harbor, these turtles are presented as sets of additional time–temperature curves in Fig. 2b. Since all 7 carcasses of each group (Kemp's ridley or green sea turtle), were placed simultaneously into the carboy and then eventually all ended up in the harbor, the time–temperature curves for each group in Fig. 2b are nearly identical. In this second group (Fig. 2b), the TTF at 20°C ranged from 2 to 6 d, but decomposition to sinking was extremely long, requiring an additional 50 to 60 d because of the exceptionally cold temperatures in the harbor. Although decomposition rates varied between species, there was overlap between species and also notable variability within species (Cook et al. 2020), and the mean carcass size (Kemp's ridley = 27.2 cm straight carapace length [SCL], green = 26.2 cm SCL) was not significantly different (p = 1.000) between species; therefore, the results of all the carcasses were treated as 1 set of 37 observations in subsequent analysis.

3.1.2. Temperature effect

The influence of temperature on decomposition and resulting TTF is apparent in the plot of the TTF against the average temperature recorded during each experiment (Fig. 3a). In all cases, temperature was relatively stable over the length of each experiment because of the controlled conditions in the tank and carboy. The data show a strong reduction in TTF at higher temperatures, with carcasses at near 20°C taking ca. 90 h to float, and carcasses maintained near 30°C taking about 30 h. A simple linear regression was fit to the data to give a relationship of TTF to temperature for the 37 experimental carcasses (Fig. 3a).

In order to apply the relationship in Fig. 3a in a backtracking model system, 2 problems must be addressed: (1) above 35°C, the linear regression falls below 0 h; and (2) there is a tendency for the carcasses maintained at 9.5 m to have a greater TTF than those at 2.2 m and shallower. The latter prediction is logical

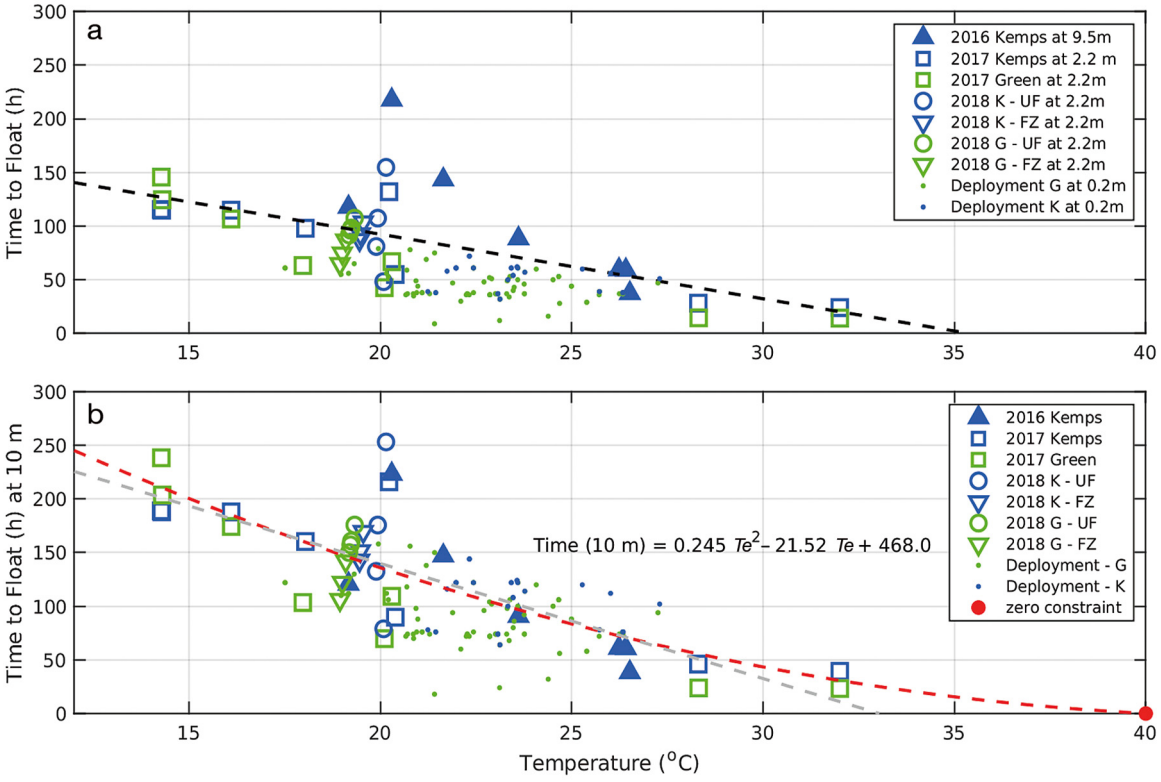

Fig. 3. Observed time to float (TTF) for 37 decomposition trials. (a) TTF at various depths. Black dashed line is a simple linear regression fit to the data, showing the relationship of TTF to temperature. (b) TTF extrapolated to a depth of 10 m. Least squares 2nd-order polynomial fit to the experimental trial data is represented by a red dashed line. The red dot marks the zero constraint point, i.e. the value through which the polynomial regression was constrained. The grey dashed line is the linear regression fit of TTF on temperature (*Te*) for the experimental trial data from (a). ▲: Kemp's ridley in the 2016 tank trials; □: Kemp's ridley in the 2017 carboy trials; □: green sea turtles in the 2017 carboy trials; ▽: 2018 frozen Kemp's ridley; ○: 2018 unfrozen Kemp's ridley; ▽: 2018 frozen green sea turtles; ○: 2018 unfrozen green sea turtles; •: deployment Kemp's ridley; •: deployment green sea turtles

based on Boyle's law where gas produced by decomposition at about 10 m would occupy a volume half that occupied at 0 m. Addressing these backtrack model problems required examining this likely pressure effect more closely.

3.1.3. Pressure effect

The spread of the residuals about the linear regression of the TTF shows that carcasses in the tank at 9.5 m (K1–K7) took up to 2 times longer to float than the other 30 carcasses at depths less than 2.2 m at the same temperature (Fig. 3a). Comparison of residuals with the Mann-Whitney test gave a low probability (p = 0.01) that this occurrence was by chance alone and led us to conclude that the departure of the carcasses at 9.5 m depth (K1–K7), from the results for the 30 carcasses maintained at 2.2 m, was primarily due to the influence of the greater pressure at 9.5 m, in this case 1.22 atm, versus 1.95 atm, a factor of 1.6×.

Based on a likely pressure effect on the TTF, the influence of pressure was compensated using Boyle's law to adjust all TTF to a standard depth, in this case a depth of 10 m. This calculation assumed that ambient pressure is directly proportional to gas production and the TTF. Fig. 3b provides a re-plotting of the 37 experimental measurements of TTF as calibrated to a standard depth of 10 m. With all carcasses plotted using the pressure-adjusted TTF, a nonlinear decrease in TTF is evident in the relationship of temperature to TTF (Fig. 3b). A polynomial regression (see Text S1 for derivation) with a zero constraint at 40°C fit the pressure adjusted data for the 37 experimental carcasses as:

$$\mathrm{TTF}(10\ \mathrm{m}) = 0.246Te^2 - 21.52Te + 468.0 \quad (1)$$

The zero constraint ensures that no values predicted by the regression would fall below zero. This polynomial is the basis of a quantitative model of time for carcasses to float based on water temperature and is employed in fitting a general model of carcass decomposition using the units of ADH. Since the TTF is a quantitative measure of decomposition, the relationship of Ratkowsky et al. (1983) is then used in detrending the decomposition rate from temperature (see Text S1) where it can be employed to integrate the environmental temperature (*Te*) over widely varying conditions using the cADH.

The polynomial regression (Eq. 1) also allows for a test of any difference in TTF between species, Kemp's ridley versus green sea turtles, by standardizing the TTF for all 37 carcasses to 20°C (in addition to the 10 m depth criteria). We found a possible difference (p = 0.1, *t*-test) with green sea turtles showing a quicker TTF than the Kemp's ridleys. However, as evident in the overlap of the data in Fig. 3b, this is not a strong difference and for the purpose of modeling, the 2 species are treated identically.

3.1.4. Decomposition: comparing ADH and cADH

The integration of temperature with time, as ADH, is shown in Fig. 4a for the 37 carcass trials where each carcass is shown as a trajectory line, gaining degree hours as time progresses. Also shown are 3 measures of the mean ADH for critical stages of decomposition related to carcass drift denoted as: 'Float' (Code 2.1), 'Peak' or maximum buoyancy (Code 3.1), and 'Sink' when the carcass sank beneath the surface (Code 3.3). A scatter of the ADH values of each stage about their means is shown in Fig. 4b. There was a trend of increasing ADH with time within each stage due to high temperatures having a greater influence on decomposition (Fig. 4a). Carcasses maintained at high temperatures trend along trajectories towards the left side of Fig. 4a, reaching a given stage sooner, while carcasses kept at cool temperatures trend towards the right-hand side, taking much longer. The result is that an equal value of ADH will give different results that are dependent on the actual ambient temperature. The overall effect is that 1 h decomposing at 30°C causes far more decomposition than 2 h at 15°C. Thus, the ADH is not successfully independent from temperature and does not sufficiently predict stage of decomposition based on ambient temperature alone.

To account for the nonlinear increase in decomposition observed at higher temperatures, we derived a cADH. Numerical detrending, in this case dividing ADH by the polynomial expressing time from temperature, gives a temperature correction (*Tc*) as:

$$Tc = \frac{2086.4}{0.246Te^2 - 21.52Te + 468.0} \quad (2)$$

where 2086.4 is the rotation point on which the detrending occurs. This point was chosen as the midpoint at 25°C for the range of temperatures, 18–32°C, that are expected when applying the decomposition model in the northern Gulf of Mexico.

The ADH values for decomposition stages were replotted using the cADH as defined in Eq. (2)

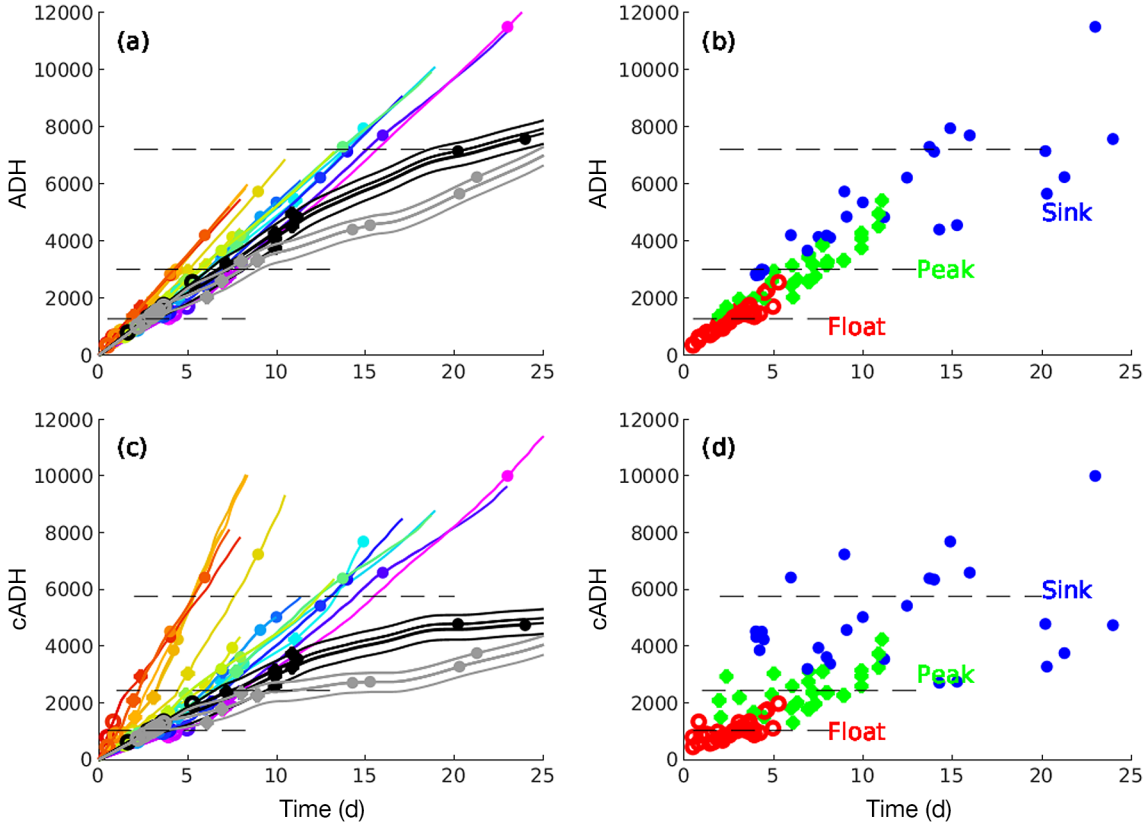

Fig. 4. Accumulated degree hours (ADH) over time (days) for the 37 experimental trials. Horizontal dashed lines indicate the mean values of time to float (Float), maximum bloat (Peak), and time of sinking (Sink). (a) Curve colors matched to initial experimental trials as per Fig. 2. (b) ADH for trials as in panel (a), but with curves removed and symbols plotted in 1 color for each time to float (red), maximum bloat (green), and time of sinking (blue). (c) Corrected ADH (cADH) for trials, with symbols and colors as in panel (a). (d) cADH for trials, with curves and symbols simplified for clarity as in panel (b)

(Fig. 4c,d). Under this calculation, cADH accumulate much more quickly at the higher temperatures and at reduced rates at the cooler temperatures. Fig. 4d also demonstrates how the temperature dependency of the decomposition is better incorporated into the calculation of the cADH as evidenced by a more uniform distribution around their mean values for each stage of floating/sinking.

3.1.5. Decomposition codes and cADH

cADH values for decomposition codes are shown in Fig. 5. Mean values and incremental values between each code are annotated on the plot. Although somewhat cluttered, the curves linking the cADH for each carcass provide a more uniform measure of decomposition than uncorrected ADH, i.e. without correcting for temperature. Based on condition code evident at the time of stranding, the corresponding mean cADH value can be used in backtrack calculations.

3.1.6. TTF calculation

As expected based on field observations, carcasses used in this study sank and required some amount of decomposition and accumulation of gas to float (Figs. 1 & 2a,b). At 1 atm (essentially the sea surface), a carcass will float once it has reached $\overline{\text{cADHf}} = 1014.9$ degree hours (see Text S1), but at greater depths, a higher value is required (greater pressure at depth). The cADH to float (cADHf) at a specific depth (Z) can be calculated as:

$$\text{cADHf}(Z) = \overline{\text{cADHf}}\left(1 + \frac{Z}{10}\right) \quad (3)$$

Incorporating the influence of the corrected temperature (Tc), TTF can be calculated as:

$$\text{TTF} = \frac{\overline{\text{cADHf}}\left(1 + \frac{Z}{10}\right)}{Tc} \quad (4)$$

The result of Eq. (4) will be the TTF (h) for a carcass that immediately sank after death.

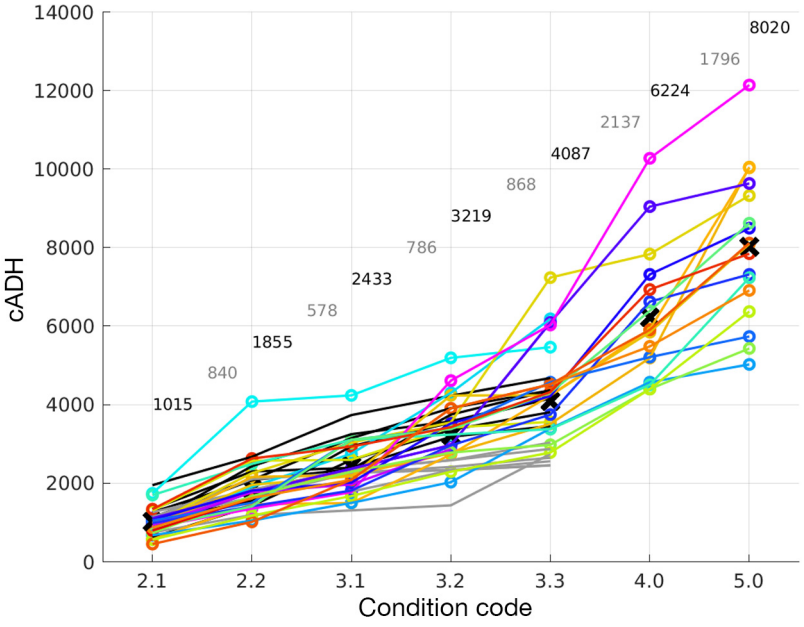

Fig. 5. Corrected accumulated degree hours (cADH) for all experimental carcasses extending from carcass condition codes 2.1 through 5 (see the Appendix for code descriptions). **Bold** numbers at the top of the curves and × symbols on the plot are the mean cADH to achieve each level of condition code, lighter numbers are the net cADH between condition codes. Curve colors are those used in Fig. 2a

3.2. Backtrack modeling

3.2.1. Integration of carcass parameters as applied in the backtrack model

Carcass decomposition and the eventual production of gas, *vg*, is a function of the environmental temperature as corrected for decomposition, *Tc* (see Text S1), and accumulates as a function of time, *t*. d*t* is the differential of time *t*. Integration of *vg*(*Tc*(*t*)) from death at *t* = 0 to the time that a carcass floats to the surface, *t* = TTF, can be represented as the integration:

$$\mathrm{cADHf} = \int_0^{TTF} vg(Tc(t))\mathrm{d}t \quad (5)$$

giving the cADH to float, cADHf.

Once a carcass reaches the sea surface (at TTF), it continues to decompose, and subsequent stages of decomposition can also be measured as the continued integration of decomposition from the moment of death to each later stage, as an STSSN code 2 (*c2*) and 3 (*c3*) respectively as:

$$\mathrm{cADH}_{c2} = \int_0^{2} vg(Tc(t))\mathrm{d}t \quad (6)$$

$$\mathrm{cADH}_{c3} = \int_0^{3} vg(Tc(t))\mathrm{d}t \quad (7)$$

and assume decomposition at these stages is related to temperature in the same way as it was for the TTF. We also measured ADH requirements for carcasses to reach STSSN codes 2 and 3, although not as precisely determined as the TTF (under camera surveillance) since judging these codes is more subjective and only monitored about every 12 h. Data suggest much faster decomposition at high temperatures as noted with other codes.

3.2.2. Backtracking formula

We applied the above relationships to determine the likely position along a backtrack route where a carcass most likely originated, i.e. death occurred. We use STSSN code 2 as an example, but STSSN code 3 can be calculated similarly. Only STSSN codes 2 and 3 are used for backtracking. While code 1 (fresh dead or mildly decomposed) could be used, in many instances carcasses in this condition strand alive and die on the beach and may not have been passively drifting as carcasses do. In addition, the postmortem interval of carcasses classified as codes 4 and 5 is highly uncertain rendering backtracking results unreliable. Those carcasses found as desiccated or skeletal remains could have drifted a great distance or may have been discovered days after beaching.

The effect of ocean temperature can be used in a degree-hour budget and deducted from the available degree-hours of a carcass along the backtrack route as:

$$\mathrm{cADH}(t') = \mathrm{cADH}_{c2} - \sum Tc(t')\Delta t \quad (8)$$

The left-hand term is the cADH along the backtrack route at time *t'*, used here to designate the reverse time steps implemented for the backtracking, Δ*t* is the time interval used for the backtracking. The cADH_{c2} is the total cADH an STSSN code 2 carcass would have accumulated upon its arrival on shore. The right-hand summation term is the summation of the temperature correction, *Tc*, along the backtrack route. When Eq. (8) solves to zero, i.e. the cADH on shore is equal to the *Tc* summed along the backtrack route, then the maximum backtrack location is achieved at which

the carcass would most likely have originated had it not initially sunk to the sea floor (i.e. the cADH = 0).

As mentioned above, at 1 atm (essentially the sea surface), a carcass will float once it has reached $\overline{\text{cADHf}} = 1014.9$ degree hours (Fig. 5), but at greater depths a higher value will be required (greater pressure at depth). In backtracking, an adjustment for actual depth (and pressure) on the sea floor is necessary. Since varying depths are found along the backtrack route, we apply Boyle's law along the backtrack route as:

$$\text{cADHf}(Z(t')) = \overline{\text{cADHf}}\left(1 + \frac{Z(t')}{10}\right) \quad (9)$$

over depths Z and time steps t', to determine the cADHf for locations on the track line.

When the backtracked budget for a carcass, cADH(t'), Eq. (8) equals the depth-compensated Boyle's law in cADHf($Z(t')$), Eq. (9), we then have an exact match for a backtrack location that is solved for both the temperature along the surface route and the influence of water depth on the TTF of a carcass as:

$$\text{cADH}(t') - \text{cADHf}(Z(t')) = 0 \quad (10)$$

The calculation of Eq. (10) is critical in solving backtracks since there are variations in water depth along the backtrack route, such as with deep bays and offshore shoals. In these cases, a decomposed carcass could originate from shallower depths further offshore, or possibly deeper depths close to shore. There may also be deep offshore locations, well beyond 30–40 m, from which the carcass likely could not originate. Thus, Eq. (10) may give more than one solution. When the solution is not perfect, but close, this information can also be used as an indicator of goodness of fit.

Since the actual measurements of carcass decomposition show considerable variation in the TTF and the cADH, we can use this variability to introduce error bounds to estimate uncertainty in comparing Eqs. (8) & (9) and provide a method of comparing the various solutions along the backtrack route. The error ranges for the STSSN code 2 and code 3 carcasses are: E_2 = 709 cADH and E_3 = 827 cADH, respectively. Probable locations of origin, Pr, for a carcass along its backtrack route (t') can then be determined as:

$$Pr(t') = \left(\frac{E - |\text{cADH}(t') - \text{cADHf}(Z(t'))|}{E}\right)^2 \quad (11)$$

where a value of 1 indicates a perfect fit, and conversely lower values tending towards zero indicate a poor fit and low likelihood.

3.3. Individual backtrack example

Carcass backtracking from beach stranding locations provides at-sea estimates of where death might have occurred. Nero et al. (2013) used ocean model-generated estimates of surface currents and winds, as well as the leeway, to directly determine the along-track coordinates, and a final endpoint based on a preset number of time steps. However, no consideration was given for ocean depth and the time required for a carcass to decompose and generate enough gas to float to the sea surface. Furthermore, no consideration was given for the possibility that carcasses in deep water might not resurface. To demonstrate the new set of routines, outlined above (Eqs. 2–11), an example backtrack is given below and 2 additional examples are provided in the supplemental material (Text S2).

A sea turtle was found on the beach as an STSSN code 2 carcass on 1 May 2019 in Waveland, Mississippi. The model first uses the ocean model currents and winds from NGOFS to backtrack for 192 h (8 d) in time (Fig. 6) in the same way as per Nero et al. (2013). The 192 h provides a reverse time sequence

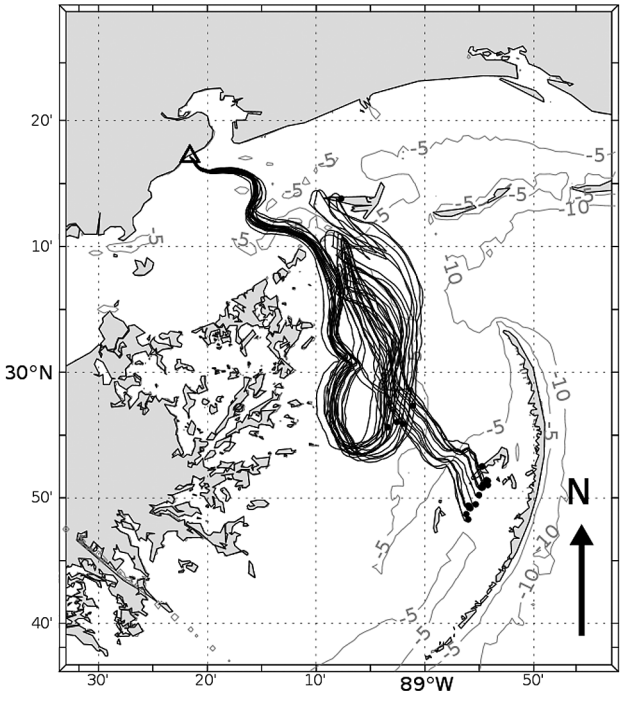

Fig. 6. Backtrack of a beach-stranded Sea Turtle Stranding and Salvage Network (STSSN) code 2 carcass; beach location is designated with a triangle. Individual lines are the ensemble of 20 random backtrack realizations produced using a 10% random walk with black dots representing the furthest track endpoints

sufficient to give an appropriate track length for most STSSN code 2 carcasses found in the northern Gulf of Mexico, while STSSN code 3 carcasses require 288 h, or 12 d.

Solving to determine where along the length of the backtrack (Fig. 6) that mortality most likely occurred is complicated, as it is dependent on both water temperature and pressure (depth). Bathymetry data provide bottom depth (Fig. 7a) and the ocean model output used for the backtracking can be simultaneously queried to provide estimates of the surface temperature (Fig. 7b, *Te*). Bottom depth is applied in Eq. (9) to determine the cADHf for various positions on the predicted track line (Fig. 7b, *Tc*).

The temperature conversion formula, Eq. (2), is then used to convert the sea surface temperature along the backtrack route, *Te*, into the form required for the decomposition calculations, *Tc* (Fig. 7b). In early May, the 22–24°C temperatures were calculated to 18–22°C temperatures, and also declined with time at earlier points along the backtrack (Fig. 7b). They also show a 24 h sawtooth pattern, the influence of the day–night heating–cooling cycle.

The cumulative sum of *Tc* along the backtrack (Fig. 8a) is then subtracted from the total cADH of the carcass as found on the beach ($cADH_{c2}$) as in Eq. (8), giving the resulting cADH for positions on the backtrack route (Fig. 8a). This curve begins at the beach, with time step 0, at 1723 cADH, and gradually declines to 0 cADH at about time step 330, (equivalent to 83 h, or 3.4 d). This decline to zero cADH is the likely timestep when the sea turtle may have died had it begun drifting without ever sinking to the sea floor. If the carcass was categorized as an STSSN code 3 upon stranding, a $cADH_{c3}$ of 3258 would be applied.

For carcasses that sink, the probable locations of origin are then determined by comparing the cADH and cADHf curves, as in Eq. (10), and

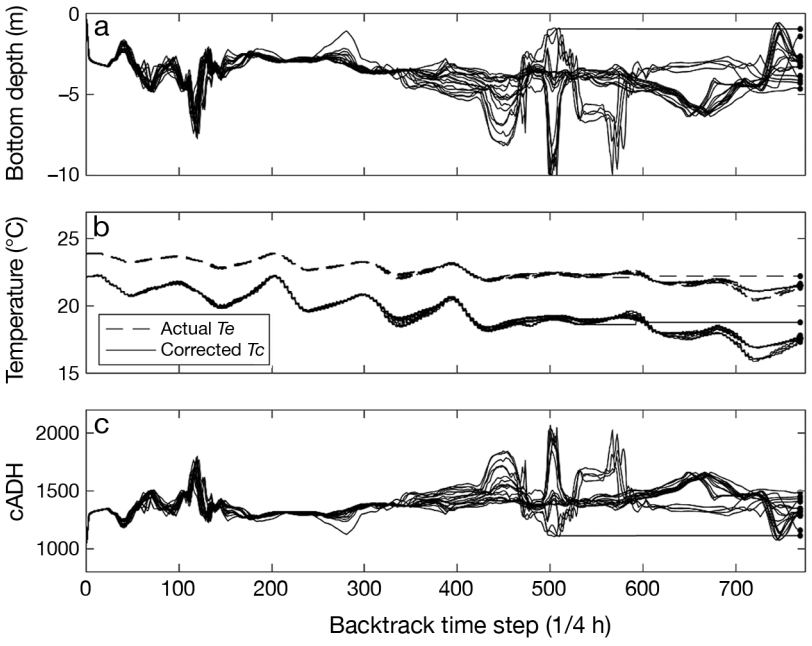

Fig. 7. Conditions along the backtrack route for a sea turtle found on the beach as an STSSN code 2 carcass on 1 May 2019 in Waveland, MS. (a) Bathymetry, (b) temperature at the sea surface along the backtrack route (*Te*) and its conversion to the corrected temperature (*Tc*), and (c) bathymetry converted to corrected accumulated degree hours (cADH) required to float along the backtrack route

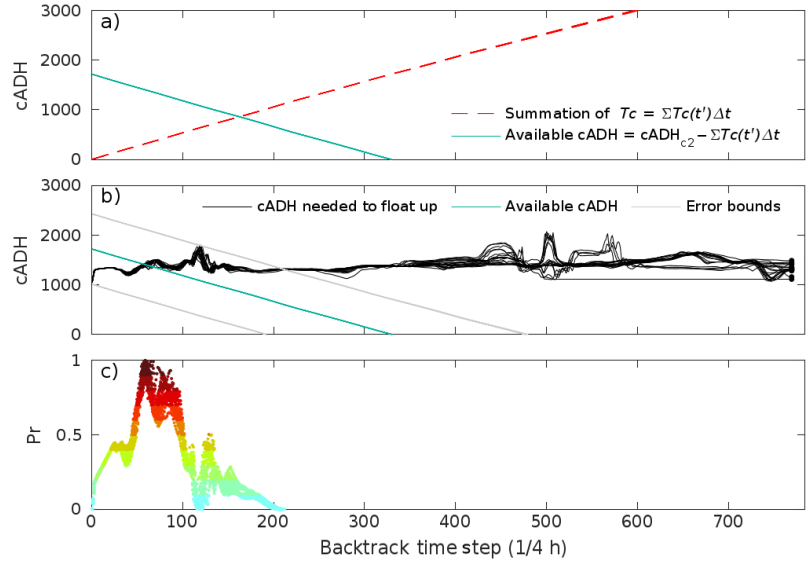

Fig. 8. (a) Calculation of the cumulative sum of *Tc* along the backtrack route (red dashed line). The subtraction of the cADH along the backtrack from the starting value of the ADH for an STSSN code 2 carcass found on the beach ($cADH_{c2}$) giving the net budget of available cADH at each point along the backtrack route is shown as a teal line. (b) An overlay of the cADH budget along the backtrack (teal line) with the cADH necessary for a carcass to float up from the sea floor (black curves) as well as the ± error bounds on the cADH budget (thin lines). The process to calculate the cADH necessary for a carcass to float up from the sea floor is shown in Fig. 7. (c) Resulting probability of origin values created from comparing the above cADH curves in (a) using Eq. (11) described in Section 3 for backtracking. Colors range from low probability (light blue) to high probability (dark red)

shown graphically in Fig. 8b. Where the cADHf and error curves cross, calculated using Eq. (10), are the backtrack time steps most likely to have been the locations of origin for the carcass, i.e. where death occurred. The solution of Eq. (11), which calculates the squared relative difference, then provides a probability, or likelihood estimate, as shown in Fig. 8c, from 0 (low) to 1 (high). The likelihood values are then co-located using the along-track latitude–longitude data to color map the original backtrack plots (Fig. 9). One optional feature for the map plots is to provide estimates of the possible source locations if the carcasses had never sunk. These locations are shown as the purple points in Fig. 9.

3.4. Drift experiments

Backtrack heatmaps of predicted source locations for the objects released at the 3 deployment sites (Cook et al. 2021) are shown in Figs. 10–12. The backtracking model predicted the original deployment locations at Sites A and B with high probability (Figs. 10 & 11, respectively). This outcome suggests that if carcasses were from an actual sea turtle mortality event, the model would accurately estimate the general area where sea turtles died. Backtracking of Site B objects centered on the deployment site while the region of high probability was just slightly inshore of Site A. Backtracking of Site C objects, which incidentally required longer time periods and distances (Fig. 12), was less accurate than the more inshore sites (Figs. 10 & 11).

4. DISCUSSION

Mortality of animals in the marine environment is by its nature often cryptic. Marine animals found on shore, i.e. stranded, present formidable challenges to biologists, wildlife managers, and other scientists who seek to understand mortality sources. These issues are particularly acute for imperiled species where strandings can generate considerable concern among stakeholders and resource agencies, as well as influence mitigation measures and other conservation actions. Determining the location where a marine animal actually died is often a critical question, as it may help link mortality with specific causes or circumstances. Predicting locations of mortality sources requires understanding of both taphonomic processes and the environmental factors that influence decomposition, as well as the dispersal and persistence of carcasses. Although there have been numerous studies on human (Mateus & Pinto 2016, Reijnen et al. 2018) and animal decomposition (Anderson & Hobischak 2004, Anderson & Bell 2014, 2016), few researchers have studied decomposition of marine animals or sea turtles in particular (Santos et al. 2018). Using cadaver studies and robust sample sizes, we show that both depth and water temperature significantly influence sea turtle decomposition, which has considerable bearing on the dispersal of dead sea turtles and thus probability of discovery.

The time required for a submerged carcass to float is a key measurement for mortality investigation. For sea turtles that sink upon death, as has been noted for important mortality sources such as fisheries bycatch, the TTF identifies the first instance that a carcass reaches the sea surface, is influenced by surface winds and oceanic currents, and is visible for discovery. Fortunately, it is also the most quantifiable and least subjective parameter observed during our decomposition trials, despite the potential for considerable variation due to species, body composition, and diet (Cook et al. 2020). We found a significant depth/pressure and temperature effect; TTF was

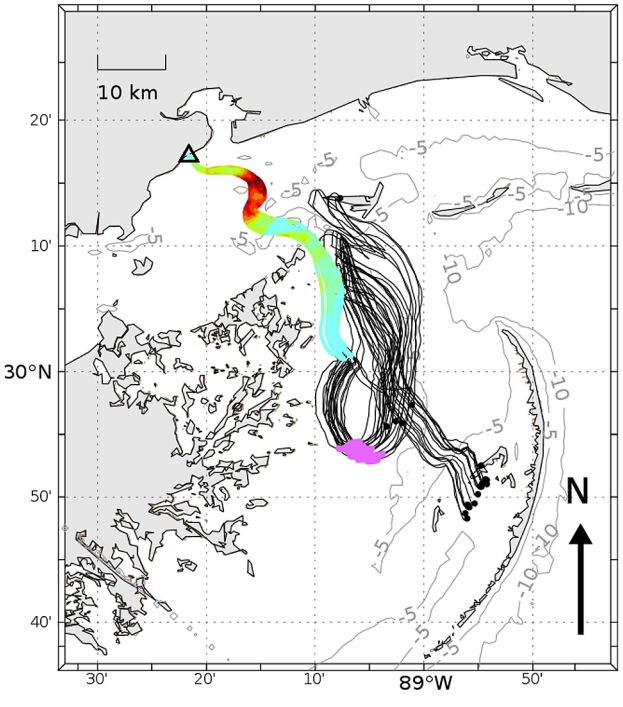

Fig. 9. Resulting probability of origin for a carcass backtracked from a beach location (triangle). Probability color range as in Fig. 8c, with addition of the possible carcass source if having never sunk (purple dots) and backtrack endpoints (black dots)

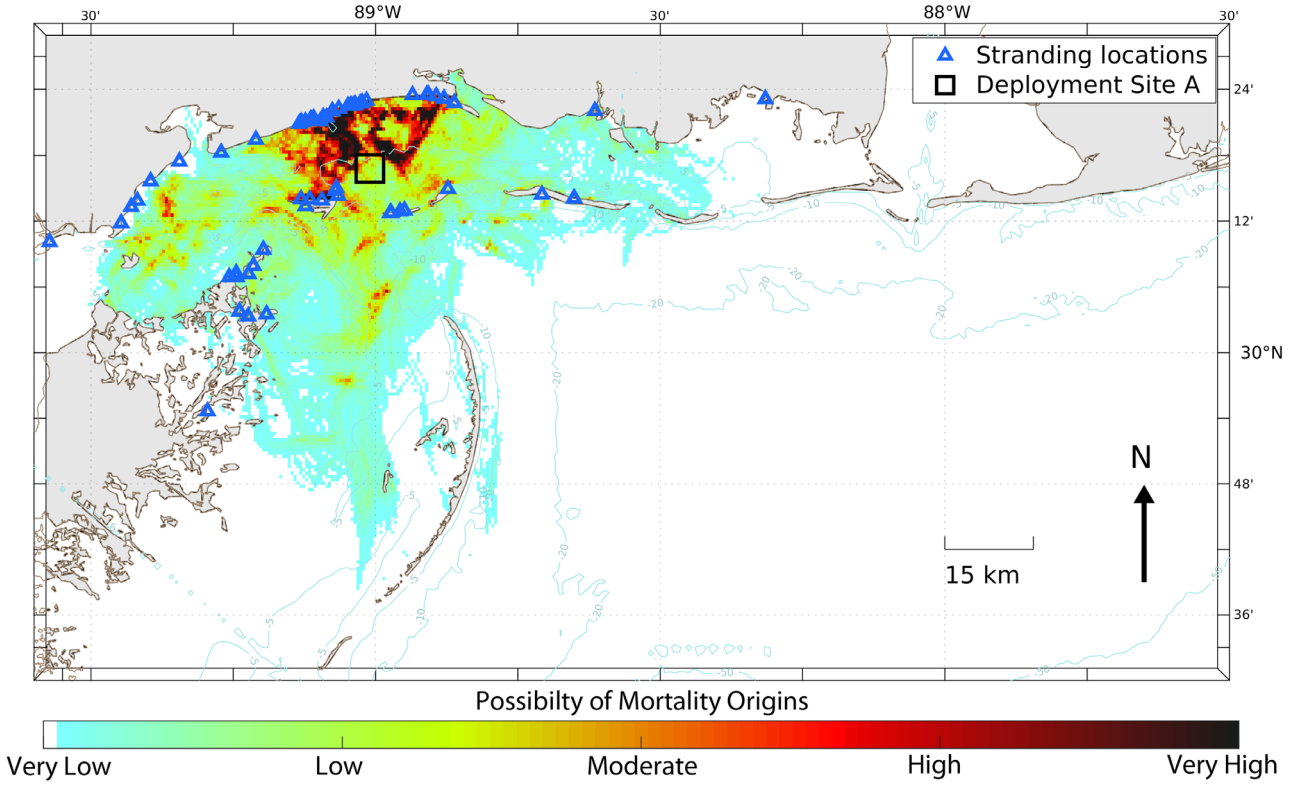

Fig. 10. Backtracking heat map generated for 63 objects (carcasses and wood block effigies) systematically deployed in 2017 from Site A (black square in the middle of Mississippi Sound) and object 'stranding' or beaching locations (blue triangles) in coastal Mississippi and eastern Louisiana. Heat map colors range from zero probability (white), through low (light blue) to high (dark red to black)

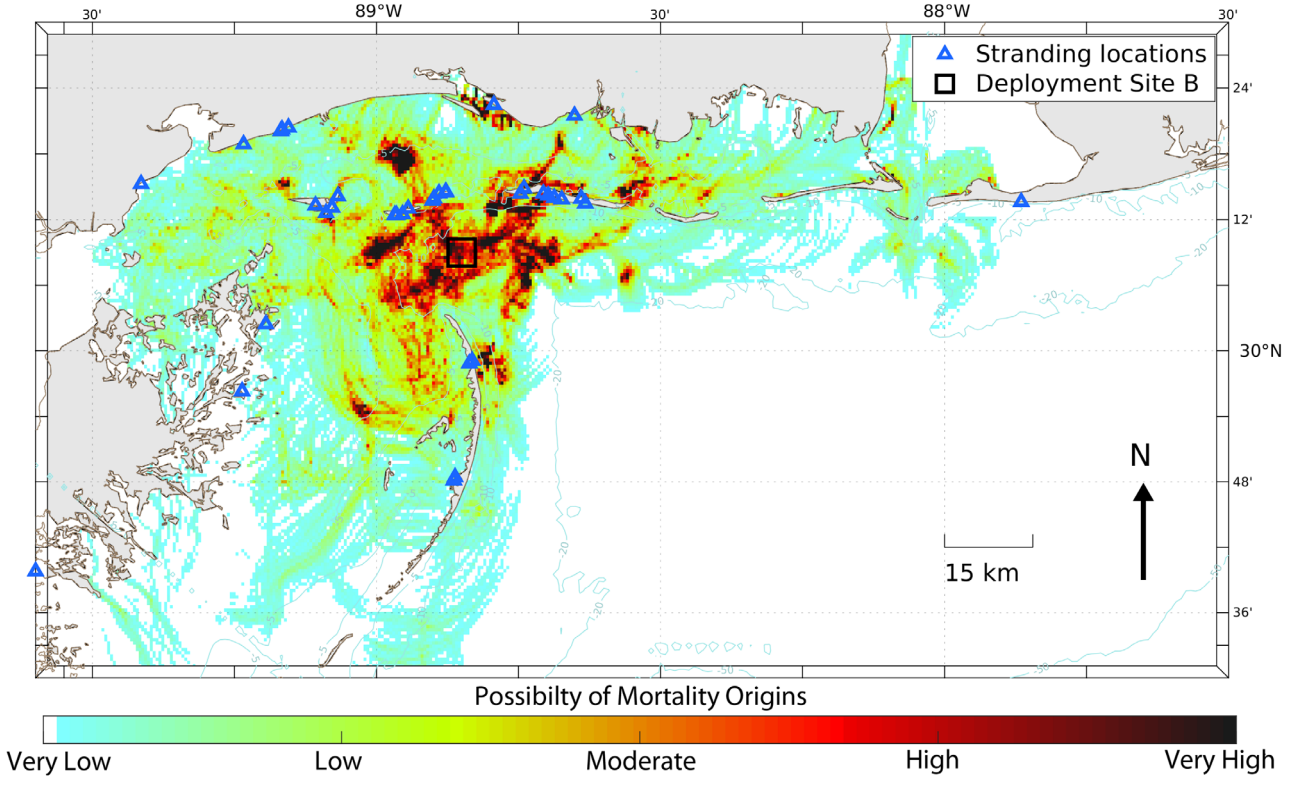

Fig. 11. As in Fig. 10, but for 39 objects (carcasses and wood block effigies) deployed from Site B (black square) just south of Ship Island

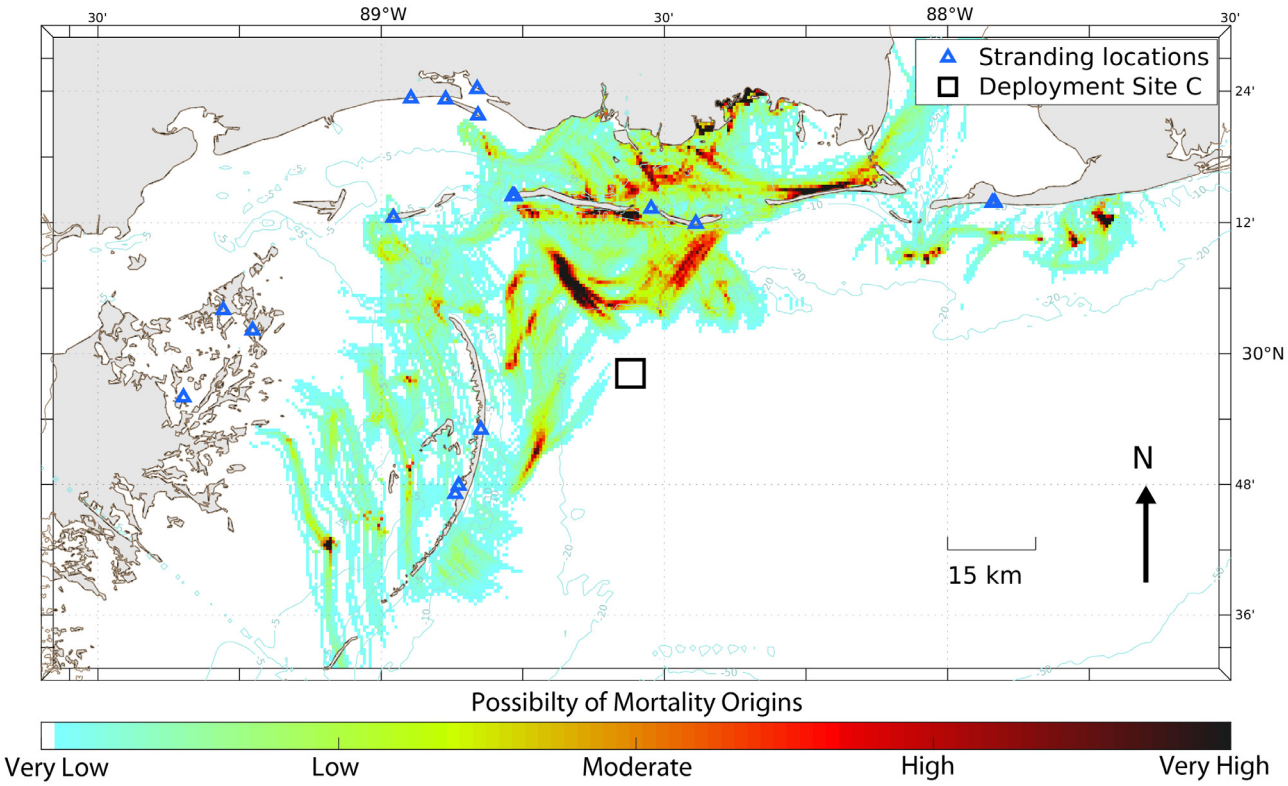

Fig. 12. As in Fig. 10, but for 18 objects (carcasses and wood block effigies) deployed from Site C (black square) in offshore waters of Mississippi

longer when incubated at colder temperatures and greater depths. The TTF followed an inverse curvilinear relationship where carcasses exposed to the coldest temperatures took 8× longer to float. The carcasses used for drift studies also illustrated this pressure effect. They were kept in small coolers (~20 cm depth) and were the quickest to float (dots in Fig. 3a that are well below the line) because they were at sea level. In the northern Gulf of Mexico, Kemp's ridley sea turtles commonly occupy habitat from nearshore waters ≤37 m to offshore regions of 50–60 m and are observed in depths up to 200 m (Shaver & Rubio 2008, Coleman et al. 2017). Green sea turtles primarily occupy nearshore, shallow waters, but will frequent deeper water seasonally or during migration (Hart & Fujisaki 2010, Shaver et al. 2013). Sea turtles have been found in water temperatures as low as 10°C, or colder depending on species (Epperly et al. 1995); thus a broad range of water temperatures and depths is relevant to studies of sea turtle mortality.

Beyond certain depth and temperature thresholds, a carcass will not generate enough gases to overcome the influences of pressure, temperature, and volume to float to the surface. We hypothesize that submerged carcasses must generate enough gas and float before they become severely decomposed (condition 3.3 at ~4000 cADH) or they will never float. At this stage, the carcass likely loses its structural integrity to the degree that it can no longer contain internal gases. Extrapolation of the TTF of 1014.95 cADH suggests this depth is between 30 and 40 m. However, temperature will also influence how long it takes for a carcass to become buoyant; therefore, outcome likely depends on both depth and associated temperatures. Our prediction seems consistent with parameters applied to submerged human bodies. The National Underwater Rescue-Recovery Institute states that humans that drown in −1 to 4°C water will not surface unless the water temperature increases. They also state that 30 m is likely the depth at which pressure and temperature cause a body to never surface (J. Sanders et al. unpubl. data). This concept is inherent in the application of Eq. (9) and our backtracking model.

There are several important considerations with regard to our experimental findings and comparisons with the natural fate of sea turtle carcasses in the environment. While the majority of our experiment was conducted in field conditions, the initial TTF occurred in a controlled laboratory setting, and thus some factors such as scavenging were not accounted for. We assume that opportunity for scavenging by benthic fauna and resulting damage to the carcass

increases with TTF duration. If a carcass is subjected to heavy scavenging and conditions result in a long TTF, it could become compromised to the degree that it cannot hold gases and never floats. Similarly, carcasses restrained underwater, such as those entangled in ghost fishing gear or other submerged debris, would never reach the surface. While these possibilities should be considered in any analysis of strandings and broader at-sea mortality, the focus of our research and model application was investigative tools to study carcasses that wash ashore.

Potential differences in decomposition and buoyancy among sea turtle species and sizes are additional considerations. Our calculations are based on data derived from Kemp's ridley and green sea turtles; however, TTF and decomposition rates would likely follow similar patterns for other species, especially those of similar size. Sea turtles used to create equations were 21.1–31.6 cm SCL due to carcass availability and the predominant size distribution of stranded sea turtles in the region of study. Sutherland et al. (2013) compared decomposition rates of large and small pigs in a terrestrial environment. Initial decomposition rates were similar for all sizes, although larger carcasses decomposed slower during the advanced stages of decomposition. Overall, smaller pig carcasses decomposed nearly 3 times faster and did not follow the same rate of progression as the larger pig carcasses (Sutherland et al. 2013). If sea turtles follow the same trend, it is possible that TTF predictions would not be impacted since floating occurs in the initial decomposition process and only latter stages would vary. However, the factors influencing the decomposition process on land and in the marine environment are very different due to the absence of insect activity. Santos et al. (2018) included 2 larger sea turtle carcasses (67 and 68 cm) in addition to 6 smaller sea turtles (26–37 cm) in their decomposition study, and did not notice a size effect. However, the coarse time resolution of their observations (days) may have masked size-related differences. Future decomposition studies with larger sea turtles are required to truly understand if body size significantly affects decomposition and buoyancy of sea turtles.

Our carcass studies provide valuable additional data on sea turtle decomposition, but our ultimate objective was to characterize key postmortem processes in order to parameterize the backtracking model. Several aspects of our approach should be considered with regard to use in mortality investigation. First, our focus was the postmortem scenario in which carcasses initially sink and become buoyant with decomposition based on our interest in the fate of sea turtles that die from sudden causes, accounts of turtles sinking upon death, limited data acquired from sea turtles that died while carrying actively transmitting satellite-enabled tags, and the general characteristics of strandings in our region (Nero et al. 2013). Aforementioned conditions in which sea turtles strand alive or float upon death require additional interpretation and assumptions, which are accommodated by the model's flexibility (Fig. 9).

The set of routines used in the model allow the incorporation of time, temperature, and bathymetry into the backtrack modeling of sea turtle carcasses. The use of TTF, as adjusted by pressure and temperature to resolve the uncertainty in the backtracks, provides an innovative solution to estimating the at-sea origin of sea turtle mortalities. Our test of the model accuracy predicted the source location of year-round deployments of 120 sea turtle effigies and carcasses, demonstrating the overall reliability of the model. The model is also able to predict the source location for carcasses that do not sink by taking the reversed cADH and searching that array for where they reach zero. These carcasses begin drifting immediately, which results in longer drift tracks. The reduced ability of the model to predict drifts with longer durations of 3–4 d, and distances of 40–50 km from shore likely reflect the additive role of random and small-scale (sub-model scale space and time) sea and weather conditions, as well as decreasing the ability of the NGOFS ocean model to give reliable backtracks over increasing time periods and steps that are inherent to longer predictions. Nonetheless, we feel that the resulting model and application are very useful, particularly for mortality within 10 km of shore, given that drifting test objects came ashore over a wide region of coastal Mississippi and eastern Louisiana (~4000 km^2).

The conversion of temperature to the cADH rather than simply using ADH is essential to our approach because the exact reverse time–temperature history of carcasses found on the beach cannot be determined until the backtrack trajectory, temperature history, and projected depth of origin are resolved. In the model, a corrected temperature was used, which made the ADH estimate independent of actual temperature. If the routines were rewritten to use a temperature-dependent ADH value for each condition code, the predicted mortality location could be erroneous if changes in temperature and depth conditions occur along the backtrack.

A few key conditions of our backtracking model must be considered, including the need to document the actual time of stranding and accurately characterize postmortem condition when a carcass first

comes ashore. For these reasons, we only apply the model in areas of regular human use or structured shoreline surveys for stranded sea turtles where both time of stranding and postmortem condition can be confidently ascertained. Photographs and information related to discovery must be carefully reviewed to ensure that data inputs are sufficient for backtracking. Currently, the STSSN does not record the actual time when the carcass was first discovered, which can introduce error into the model. To account for the range of possible times when the carcass may have beached on the day it was reported, the model is run at five 6 h intervals (0, 6, 12, 18, and 24) to produce a spaghetti plot of possible drift tracks.

Backtracking accuracy also relies on accurate assignment of postmortem condition code upon stranding, which requires careful validation. While carcasses are floating, decomposition rates are driven primarily by water temperature because water has a higher specific heat conductivity than air. However, once carcasses beach, sunlight and the temperature of the sand can greatly affect decomposition rates. During summer months, if a carcass is not found within hours of beaching, it will quickly decompose, which typically results in a longer drift track than would be predicted if carcass condition was determined when it first came ashore. As with time of stranding, confidence in condition code upon stranding may simply be too uncertain for application in remote or irregularly surveyed locations. To overcome these issues, the model can be run using a range of input parameters (i.e. times, condition codes) for circumstances where lesser degrees of confidence are still useful.

Currently, only sea turtles with condition codes 1, 2, or 3 are simulated in the model to ensure the most accurate outputs. It is not possible to accurately estimate the mortality location for a dried carcass or skeletal remains because the postmortem interval is potentially very long and too uncertain. Also, we developed the parameters of our model based on postmortem condition classification criteria currently used by the STSSN in order to maximize applicability; however, a more detailed system of carcass categorization described by Reneker et al. (2018) provides more highly resolved backtrack calculations and better estimates of likely at-sea mortality locations.

An additional factor that may be significant in some regions is bottom drift, which is not incorporated into our model. Evidence from research in the northern Gulf of Mexico suggests that bottom drift plays a minimal role in overall carcass movement as compared to wind and current forcing at the sea surface. Nero et al. (2013) found that a deceased satellite-tagged Kemp's ridley drifted 1.4 km between its final transmission before death and its resurfacing 5 d later. The Argos location class errors could also account for some discrepancy in location just before death as these can range up to 1.5 km or potentially greater (CLS 2016). In addition, we have monitored 42 sea turtle carcasses placed on the seafloor in non-anchored cages in the northern Gulf of Mexico as part of additional decomposition studies and have observed very limited movement (E. Schultz pers. obs.). Thus, we do not feel that subsurface drift majorly influences carcass dispersal in this region, but should be considered if this model is applied in regions where stronger bottom currents occur.

In conclusion, we provide time–temperature relationships for stages of decomposition and key postmortem events that are relevant to backtracking of dead stranded sea turtles in order to predict the area where they died. The intent of this work is to provide the best possible estimates of mortality source locations using ocean models as described by Nero et al. (2013) and enhanced with ambient pressure derived from ocean bathymetry and corrected temperature. Our approach may be adapted to other regions where suitable ocean circulation models are available. As in the northern Gulf of Mexico, we encourage the use of appropriate drifter studies to evaluate model performance.

Acknowledgements. We thank the many staff and volunteers from the Massachusetts, Mississippi, Texas, and North Carolina Sea Turtle Stranding and Salvage Network (STSSN) for salvaging and shipping carcasses during several seasons (2016, 2017, and 2018). Without their dedication and response effort this study would not have been possible. We also thank the staff and patrons of the Bay-Waveland Yacht Club for the use of their facility. This research was supported with Sea Turtle Early Restoration Project funds administered by the Deepwater Horizon Natural Resource Damage Assessment Regionwide Trustee Implementation Group. Sea turtle research was authorized under DOI USFWS TE 676395-5 issued to the Southeast Fisheries Science Center (PI: Dr. Bonnie J. Ponwith) and USFWS designated agent letter issued to M.C. This study was also partially supported by NOAA National Centers for Environmental Information and NOAA grant 363541-191001-021000 (Northern Gulf Institute) at Mississippi State University. Mention of trade names or commercial companies is for identification purposes only and does not imply endorsement by the National Marine Fisheries Service, NOAA.

LITERATURE CITED

Anderson GS, Bell LS (2014) Deep coastal marine taphonomy: investigation into carcass decomposition in the Saanich Inlet, British Columbia using a baited camera. PLOS ONE 9:e110710

Anderson GS, Bell LS (2016) Impact of marine submergence and season on faunal colonization and decomposition of pig carcasses in the Salish Sea. PLOS ONE 11:e0149107

Anderson GS, Hobischak NR (2004) Decomposition of carrion in the marine environment in British Columbia, Canada. Int J Legal Med 118:206–209

CLS (2016) Argos user's manual. https://www.argos-system.org/wp-content/uploads/2016/08/r363_9_argos_users_manual-v1.6.6.pdf (accessed 21 April 2021)

Coleman AT, Pitchford JL, Bailey H, Solangi M (2017) Seasonal movements of immature Kemp's ridley sea turtles (*Lepidochelys kempii*) in the northern Gulf of Mexico. Aquat Conserv 27:253–267

Cook M, Reneker JL, Nero RW, Stacy BA, Hanisko DS (2020) Effects of freezing on decomposition of sea turtle carcasses used for research studies. Fish Bull 118:268–274

Cook M, Reneker JL, Nero RW, Stacy BA, Hanisko DS, Wang Z (2021) Use of drift studies to understand seasonal variability in sea turtle stranding patterns in Mississippi. Front Mar Sci 8:659536

Epperly S, Braun Mcneill J, Chester A, Cross F, Merriner J, Tester P (1995) Winter distribution of sea turtles in the vicinity of Cape Hatteras and their interactions with the summer flounder trawl fishery. Bull Mar Sci 56:547–568

Epperly SP, Braun J, Chester AJ, Cross FA, Merriner JV, Tester PA, Churchill JH (1996) Beach strandings as an indicator of at-sea mortality of sea turtles. Bull Mar Sci 59:289–297

García-Párraga D, Crespo-Picazo JL, Bernaldo de Quirós Y, Cervera V and others (2014) Decompression sickness ('the bends') in sea turtles. Dis Aquat Org 111:191–205

Hart KM, Fujisaki I (2010) Satellite tracking reveals habitat use by juvenile green sea turtles *Chelonia mydas* in the Everglades, Florida, USA. Endang Species Res 11:221–232

Mateus M, Pinto L (2016) Report on the accumulated degree days and post mortem submersion interval for an infant drowning accident. J Forensic Investig 4:3

Megyesi MS, Nawrocki SP, Haskell NH (2005) Using accumulated degree-days to estimate the postmortem interval from decomposed human remains. J Forensic Sci 50: 618–626

Nero RW, Cook M, Coleman AT, Solangi M, Hardy R (2013) Using an ocean model to predict likely drift tracks of sea turtle carcasses in the north central Gulf of Mexico. Endang Species Res 21:191–203

Parga ML, Crespo-Picazo JL, Monteiro D, García-Párraga D and others (2020) On-board study of gas embolism in marine turtles caught in bottom trawl fisheries in the Atlantic Ocean. Sci Rep 10:5561

Ratkowsky DA, Lowry RK, McMeekin TA, Stokes AN, Chandler RE (1983) Model for bacterial culture growth rate throughout the entire biokinetic temperature range. J Bacteriol 154:1222–1226

Reijnen G, Gelderman HT, Grotebevelsborg BFO, Reijnders UJ, Duijst WL (2018) The correlation between the Aquatic Decomposition Score (ADS) and the post-mortem submersion interval measured in Accumulated Degree Days (ADD) in bodies recovered from fresh water. Forensic Sci Med Pathol 14:301–306

Reneker JL, Cook M, Nero RW (2018) Preparation of fresh dead sea turtle carcasses for at-sea drift experiments. NOAA Tech Memo NMFS-SEFSC-731

Santos BS, Kaplan DM, Friedrichs MA, Barco SG, Mansfield KL, Manning JP (2018) Consequences of drift and carcass decomposition for estimating sea turtle mortality hotspots. Ecol Indic 84:319–336

Shaver DJ, Rubio C (2008) Post-nesting movement of wild and head-started Kemp's ridley sea turtles *Lepidochelys kempii* in the Gulf of Mexico. Endang Species Res 4: 43–55

Shaver DJ, Hart KM, Fujisaki I, Rubio C, Sartain AR (2013) Movement mysteries unveiled: spatial ecology of juvenile green sea turtles. In: Lutterschmidt WI (ed) Reptiles in research: investigations of ecology, physiology, and behavior from desert to sea. Nova Science Publishers, Inc, Hauppauge, NY, p 463–483

Sutherland A, Myburgh J, Steyn M, Becker PJ (2013) The effect of body size on the rate of decomposition in a temperate region of South Africa. Forensic Sci Int 231: 257–262

Vass AA (2001) Beyond the grave — understanding human decomposition. Microbiol Today 28:190–193

Appendix. Sea turtle condition codes used to classify carcasses upon retrieval, reprinted with permission from Reneker et al. (2018)

The sea turtle condition codes used for the carcass drift study are as follows.

(1) Fresh dead (Ratkowsky et al. 1983)
Carcass typically not floating, may have rigor mortis, eyes should be clear, no evidence of bloating, no odor.

(2.1) Early moderately decomposed
Carcass barely floating, less than 50% of carapace exposed above the waterline, head typically below waterline, mild bloat, very little decomposition of skin, little to mild smell.

(2.2) Late moderately decomposed
Carcass floating well, 50 to <90% of carapace exposed above the waterline, head partially exposed, moderate bloat, bulging eyes, scutes and skin may be beginning to slough, moderate smell.

(3.1) Early severely decomposed
Carcass reaches maximum floatation, 90–100% of carapace exposed above the waterline, head and neck severely distended and visible above waterline, mouth often open, severe bloat, skin on head and limbs tight, possibly a few loose scutes, carcass has not degassed and all structures are intact, strong smell.

(3.2) Mid severely decomposed
Degassing begins and carcass begins to sink, less than 90% of carapace exposed above the waterline, head and neck limp and beginning to sink, post severe bloat, scutes and skin sloughing and disarticulation beginning, skin and limbs are becoming loose, foul smell.

(3.3) Late severely decomposed
Carcass has sunk, or if floating, sinks when disturbed or flipped over due to holes in the body cavity, carcass is completely degassed, severe decomposition and sloughing of scutes and skin, disarticulation of joints and carapace, foul smell.

(4) Dried carcass (Ratkowsky et al. 1983)
Completely desiccated, only dry skin and bones, little to no smell.

(5) Bones (Ratkowsky et al. 1983)
Carcass has decomposed to bones, no soft tissue remaining, little to no smell.

Editorial responsibility: Eric Gilman, Honolulu, Hawaii, USA
Reviewed by: D. Monteiro and 2 anonymous referees

Submitted: May 21, 2021
Accepted: September 28, 2021
Proofs received from author(s): January 3, 2022